IVYSPRING INTERNATIONAL PUBLISHER

Theranostics

2018; 8(9): 2435-2446. doi: 10.7150/thno.22144

Research Paper

Harmine enhances type H vessel formation and prevents bone loss in ovariectomized mice

Jie Huang[1,4*], Hao Yin[1,4*], Shan-Shan Rao[1,6], Ping-Li Xie[7], Xu Cao[8], Tai Rao[9], Shu-Ying Liu[10], Zhen-Xing Wang[1], Jia Cao[1], Yin Hu[1,4], Yan Zhang[1], Juan Luo[1], Yi-Juan Tan[1], Zheng-Zhao Liu[1,5], Ben Wu[1], Xiong-Ke Hu[1], Tuan-Hui Chen[1], Chun-Yuan Chen[1]✉ and Hui Xie[1,2,3,4,5,11]✉

1. Movement System Injury and Repair Research Center, Xiangya Hospital, Central South University, Changsha, Hunan 410008, China.
2. Hunan Key Laboratory of Organ Injury, Aging and Regenerative Medicine, Changsha, Hunan 410008, China.
3. Department of Sports Medicine, Xiangya Hospital, Central South University, Changsha, Hunan 410008, China.
4. Department of Orthopedics, Xiangya Hospital, Central South University, Changsha, Hunan 410008, China.
5. National Clinical Research Center for Geriatric Disorders, Xiangya Hospital, Central South University, Changsha, Hunan 410008, China.
6. Department of Spine Surgery, Xiangya Hospital, Central South University, Changsha, Hunan, 410008, China.
7. Department of Forensic Science, School of Basic Medical Sciences, Central South University, Changsha, Hunan 410013, China.
8. Department of Orthopaedic Surgery, Johns Hopkins University School of Medicine, Baltimore, Maryland 21205, USA
9. Department of Clinical Pharmacology, Xiangya Hospital, Central South University, Changsha, Hunan 410008, China.
10. The Second Xiangya Hospital, Central South University, Changsha, Hunan 410008, China.
11. China Orthopedic Regenerative Medicine Group (CORMed), Changsha, Hunan 410008, China.

* these authors contributed equally to this work.

✉ Corresponding authors: Hui Xie: huixie@csu.edu.cn; Chun-Yuan Chen: chency19@csu.edu.cn; #87 Xiangya Road, Changsha, Hunan 410008, China.

Received: 2017.07.29; Accepted: 2018.02.07; Published: 2018.03.28

Abstract

Recently, researchers identified a distinct vessel subtype called type H vessels that couple angiogenesis and osteogenesis. We previously found that type H vessels are reduced in ovariectomy (OVX)-induced osteoporotic mice, and preosteoclasts are able to secrete platelet-derived growth factor-BB (PDGF-BB) to stimulate type H vessel formation and thereby to promote osteogenesis. This study aimed to explore whether harmine, a β-carboline alkaloid, is capable of preventing bone loss in OVX mice by promoting preosteoclast PDGF-BB-induced type H vessel formation.

Methods: The impact of harmine on osteoclastogenesis of RANKL-stimulated RAW264.7 cells was verified by gene expression analysis and tartrate-resistant acid phosphatase (TRAP) staining. Enzyme-linked immunosorbent assay (ELISA) was conducted to test PDGF-BB production by preosteoclasts. A series of angiogenesis-related assays *in vitro* were performed to assess the pro-angiogenic effects of the conditioned media from RANKL-stimulated RAW264.7 cells treated with or without harmine. Meanwhile, the role of PDGF-BB in this process was determined. *In vivo*, OVX mice were intragastrically administrated with harmine emulsion or an equal volume of vehicle. 2 months later, bone samples were collected for μCT, histological, immunohistochemical and immunofluorescent analyses to evaluate bone mass, osteogenic and osteoclastic activities, as well as the numbers of type H vessels. Bone marrow PDGF-BB concentrations were assessed by ELISA.

Results: Exposure of RANKL-stimulated RAW264.7 cells to harmine enhanced the formation of preosteoclasts and the production of PDGF-BB. Harmine augmented the ability of RANKL-stimulated RAW264.7 cells to promote angiogenesis of endothelial cells, whereas the effect was blocked by PDGF-BB inhibition. *In vivo*, the oral administration of harmine emulsion to OVX mice resulted in enhanced trabecular bone mass and osteogenic responses, increased numbers of preosteoclasts, as well as reduced numbers of osteoclasts and fat cells. Moreover, OVX mice treated with harmine exhibited higher levels of bone marrow PDGF-BB and much more type H vessels in bone.

Conclusion: Harmine may exert bone-sparing effects by suppression of osteoclast formation and promotion of preosteoclast PDGF-BB-induced angiogenesis.

Key words: harmine, preosteoclast, PDGF-BB, angiogenesis, osteogenesis

Introduction

Bone is a highly vascularized tissue enriched in large vessels and capillaries. During development of the mammalian skeletal system, osteogenesis is closely connected with the growth of blood vessels [1, 2]. Blood vessel networks provide access to the delivery of nutrients, oxygen, pluripotent cells and minerals, which is necessary for osteogenesis [3-5]. Recent studies revealed that a distinct capillary subtype called type H, characterized by high expression of the endothelial markers CD31 and endomucin ($CD31^{hi}Emcn^{hi}$), couples angiogenesis and osteogenesis [6, 7]. However, this specific vessel subtype is reduced with ageing, coinciding with reduced osteoprogenitor numbers and loss of bone mass [6, 8]. Our previous study showed that type H vessels are also decreased in the bone of ovariectomy (OVX)-induced osteoporotic mouse model and platelet-derived growth factor-BB (PDGF-BB) secreted by preosteoclasts can induce type H vessel generation and subsequently stimulate bone formation [9], suggesting that increasing the numbers of preosteoclasts and type H vessels are promising therapeutic strategies for osteoporosis.

Harmine, a natural tricyclic β-carboline alkaloid, is widely distributed in plants, animals, as well as in human tissues and body fluids [10]. It has a diverse range of biological activities including potent effects on skeletal and central nervous systems [11-15]. Previous studies have indicated that harmine has the ability to inhibit the fusion of preosteoclasts into multinucleated osteoclasts [11] and the intraperitoneal administration of harmine is sufficient to suppress bone resorption and prevent bone loss in OVX-induced osteoporotic mice [12]. Considering our previous study showing that preosteoclasts are capable of secreting PDGF-BB to stimulate type H vessel formation and thereby to enhance osteogenesis [9], we supposed that the promotion of preosteoclast PDGF-BB-induced angiogenesis might be an important mechanism through which harmine prevents osteoporosis.

In this study, we explored whether harmine could augment the ability of RANKL-stimulated osteoclast precursor RAW264.7 cells to promote angiogenesis of endothelial cells *in vitro* by increasing preosteoclast accumulation and PDGF-BB production. *In vivo*, harmine was prepared into an oil-in-water oral emulsion to reduce its side effects on the central nervous system and was then intragastrically administrated to OVX mice to verify the effects of harmine on type H vessel and bone formation. This study was undertaken to determine whether a harmine emulsion can be used as a therapeutic agent for osteoporosis by inhibition of osteoclast formation and promotion of preosteoclast PDGF-BB-induced angiogenesis and subsequent osteogenesis.

Materials and methods

Cell culture

The macrophage cell line RAW264.7 cells were cultured in high glucose DMEM (Gibco BRL, Grand Island, USA) supplemented with 10% FBS (Gibco) and 1% penicillin-streptomycin (Gibco). Human microvascular endothelial cells (HMECs) were cultured in MCDB131 medium (Gibco) containing 10% FBS (Gibco), 1 μg/mL hydrocortisone (Sigma, St. Louis, MO, USA), 2 mM L-glutamine (Sigma) and 10 ng/mL epidermal growth factor (EGF; Sigma). Cells were cultured at 37 °C in a humidified atmosphere with 5% CO_2.

Preparation of conditioned media (CM)

RAW264.7 cells were seeded into 48-well culture plates at a density of 1.5×10^4/well and treated with 100 ng/mL receptor activator for nuclear factor κB ligand (RANKL) and 3 μg/mL harmine or an equal volume of vehicle (DMSO). Cells cultured in high glucose DMEM supplemented with 10% FBS and an equal volume of DMSO were served as the negative controls (un-induced group). After 6 days of induction, the CM from un-induced, RANKL-treated or RANKL + harmine-treated RAW264.7 cells were harvested and centrifuged at 2000 ×g for 10 min to collect the supernatant, which was stored at –80 °C or used for downstream experiments.

Tartrate-resistant acid phosphatase (TRAP) staining

Cells were fixed with 4% paraformaldehyde for 10 min, washed three times with distilled water and then stained for TRAP using a commercial kit (Sigma) according to the manufacturer's protocol. $TRAP^+$ mononuclear cells and multinucleated cells containing at least three nuclei were identified as preosteoclasts and osteoclasts, respectively, and counted under an inverted microscope (Leica DMI6000B, Solms, Germany).

Angiogenesis-related assays *in vitro*

To test whether harmine could augment the pre-angiogenic ability of RANKL-stimulated RAW264.7 cells by promoting PDGF-BB production, HMECs were cultured in MCDB131 medium under different treatment conditions: 1) $CM^{Vehicle}$ + IgG group (treated with CM from un-induced RAW264.7 cells and isotype IgG); 2) CM^{RANKL} + IgG group (treated with CM from RANKL-treated RAW264.7 cells and isotype IgG); 3) $CM^{RANKL + Harmine}$ + IgG group (treated with CM from RANKL + harmine-treated

RAW264.7 cells and isotype IgG); 4) $CM^{RANKL + Harmine}$ + PDGF-BB Ab group (treated with CM from RANKL + harmine-treated RAW264.7 cells and PDGF-BB-neutralizing antibody). To test the direct effect of harmine on the angiogenic activities of endothelial cells, HMECs were treated with 3 μg/mL harmine or vehicle (DMSO). The IgG isotype control antibody was obtained from Abcam (Cambridge, Cambs, Britain). PDGF-BB-neutralizing antibody was purchased from R&D system (Minneapolis, MN, USA).

Tube formation assay

HMECs (1.5×10^4 cells per well) were seeded onto Matrigel-coated 96-well plates and cultured in MCDB131 medium under different treatment conditions. 6 h later, cells were observed with an inverted microscope (Leica). All the parameters (total tube length, total loops and total branching points) revealing the ability of HMECs to form tubes were measured by Image-Pro Plus 6 software.

Cell proliferation assay

A cell counting kit-8 (CCK-8; Dojindo, Kumamoto, Japan) was used to test the proliferation of HMECs in accordance with the manufacturer's instructions. Briefly, HMECs (5×10^3 cells per well) were seeded onto 96-well plates and cultured in MCDB131 medium under different treatment conditions. The wells without cells served as the blank. Each well was subjected to CCK-8 solution (10 μL per well) on day 1 to day 5, and cells were incubated at 37 °C for 3 h. The absorbance value of each well was measured at 450 nm using a microplate reader (Bio-Rad 680). The culture medium supplemented with CM from different groups, harmine, or vehicle (DMSO) was replenished every day. A growth curve was drawn to evaluate the cell proliferation rate.

Migration assay

For the scratch wound assay, HMECs were seeded into a 12-well culture plate at a density of 2.0×10^5/well and cultured until confluence. Next, the confluent cells were wounded by scratching the monolayer with a sterile pipette tip under an inverted microscope (Leica). Cells were then incubated in MCDB131 medium under different treatment conditions. Images of the wounds were acquired immediately, 6 h and 12 h later. The rate of migration area was calculated as described previously [16]: Migration area (%) = $(A_0 - An)/A_0 \times 100$, where A_0 represents the area of initial wound area, and An represents the residual area of wound at the metering point.

For the transwell migration assay, HMECs were suspended at a density of 1×10^4/well and loaded into the top chamber of a 24-well, 8 μm pore-size transwell plate (Corning, NY, USA). Then, complete medium containing CM from different groups with PDGF-BB-neutralizing antibody or isotype IgG was added to the lower chamber. After 12 h, un-migrated cells that remained in the upper chambers were removed by wiping the top of the insert membranes with cotton swabs, while the migrated cells that passed through the membrane pores were stained with 0.5% crystal violet for several minutes and counted under an optical microscope (Leica).

Quantitative real-time PCR (qRT-PCR) analysis

Total RNA was extracted using TRIzol Reagent (Invitrogen, Carlsbad, CA) and cDNA was synthesized from 1 μg of total RNA by using the RevertAid First Strand cDNA Synthesis kit (Fermentas, Burlington, Canada). Next, qRT-PCR was performed using FastStart Universal SYBR Premix ExTaq™ II (Takara Biotechnology, Japan) on an ABI PRISM® 7900HT System (Applied Biosystems, Foster City, USA). Relative gene expression was calculated by the $2^{-\triangle\triangle CT}$ method and GAPDH was used as reference for normalization. Primer sequences used for qRT-PCR were as follows: *Atp6v0d2*: forward, 5'-AGCAAAGAAGACAGGGAG-3', and reverse, 5'-CAGCGTCAAACAAAGG-3'; *Ctsk*: forward, 5'-GCGGCATTACCAACAT-3', and reverse, 5'-CTGGAAGCACCAACGA-3'; *Pdgf-bb*: forward, 5'-CCTCGGCCTGTGACTAGAAG-3', and reverse, 5'-CCTTGTCATGGGTGTGCTTA-3'; *Gapdh*: forward, 5'-CACCATGGAGAAGGCCGGGG-3', and reverse, 5'-GACGGACACATTGGGGGTAG-3'.

Preparation of harmine emulsion

Harmine emulsion was prepared by homogenizing 31.7% (v/v) distilled water in 63.2% (v/v) soybean oil with 5.1% (v/v) emulsifier solution (including 3.0% v/v Span 80 and 2.1% v/v Tween 80; HLB=10.59). Briefly, 37.5 g of harmine was dissolved in 19.02 mL soybean oil, followed by the addition of 37.92 mL distilled water, 1.8 mL Span 80 and 1.26 mL Tween 80. After mixing for 7 min at 75 °C, the mixture was passed through a homogenizing apparatus called a colloidal mill (Langtong Machinery Co.,Ltd, Hebei, China) to form uniform, dispersed and small emulsified particles. The emulsion sample was diluted in distilled water at a ratio of 1:3 and photographed under an optical microscope. The mean length diameter was calculated.

Animals and treatments

Animal care and experimental procedures were approved by the Animal Research Committee of Central South University. Thirty 12-week-old female

C57BL/6 mice (weighing 25-30 g) were used in this study. The mice were randomly and averagely divided into three groups as follows: (1) sham group (served as controls and treated with an equal volume of vehicle); (2) model group (mice subjected to bilateral OVX and treated with vehicle); (3) harmine group (mice underwent OVX and treated with harmine emulsion). Briefly, mice were generally anesthetized and subjected to OVX or a sham operation as described previously [9, 17, 18]. Two weeks later, harmine emulsion (10 mg/kg) was intragastrically administrated to the mice in the harmine group. The mice in the model group and in the sham group were oral gavaged with an equal volume of vehicle (emulsion without harmine). The treatments were conducted daily for 2 months. Bone marrow samples from tibias of mice were collected in heparin and centrifuged at 860 ×g for 10 min to obtain the supernatant, which was stored at –80 °C until analyses. Uteri were isolated and weighed to confirm the success of OVX and femora were collected for further analyses.

Microcomputed tomography (μCT) analysis

Femora were dissected from mice, fixed in 4% paraformaldehyde for 48 h and analyzed by Skyscan 1176 (Skyscan, Aartselaar, Belgium). The scanner was set at a voltage of 50 kV, a current of 400 μA and a resolution of 8.88 μm per pixel. A trabecular bone region of interest (ROI) was drawn starting from 0.15 mm proximal to the distal epiphyseal growth plate and extended proximally for 0.4 mm in order to determine the trabecular bone volume fraction (Tb. BV/TV), trabecular thickness (Tb. Th), trabecular number (Tb. N) and trabecular separation (Tb. Sp).

Histological, immunohistochemical, and immunofluorescent analyses

For histological and immunohistochemical analyses, femora were dissected and fixed in 4% paraformaldehyde for 48 h, decalcified in 10% ethylene diamine tetraacetic acid (EDTA; pH=7.4) for 21 days, dehydrated through graded ethanol of increasing concentration and then embedded in paraffin. Samples were cut into 5 μm thick longitudinally oriented sections and processed for hematoxylin and eosin (H&E) staining, osteocalcin (OCN) immunohistochemistry staining and TRAP staining as described previously [9]. Images were acquired with an optical microscope (CX31; Olympus, Hamburg, Germany). Positively stained cells or relative staining intensity were measured in three random visual fields per section, three sections per mouse and three or four mice per group. For H&E and TRAP staining, the numbers of adipocytes per square millimeter of bone marrow area (N/mm^2), and preosteoclasts or osteoclasts per adjacent bone surface (N/mm) were calculated. TRAP staining kit was purchased from Sigma. OCN antibody and the secondary antibody were obtained from Abcam.

CD31 and Emcn double immunofluorescent staining were performed to evaluate the extent of type H vessel formation and conducted as previously described [9]. Briefly, fresh femora were removed and immediately fixed in 4% paraformaldehyde for 4 h, followed by fast decalcification in 18% EDTA for 3 days. Subsequently, the samples were dehydrated in 30% sucrose, embeded in OCT and cut into 30 μm thick longitudinally oriented sections of bone including the metaphysis and diaphysis. Bone sections were then stained with primary antibodies overnight at 4 °C and with the secondary antibodies at room temperature for 1 h. Sections incubated with secondary antibodies alone served as the negative controls. Nuclei were stained with DAPI. Images were acquired with a Leica DMI6000B fluorescence microscope (Solms, Germany). The numbers of type H vessels (HV) and total vessels (TV; positive for Emcn) were determined by three random fields per section, three sections per mouse and four mice per group. The percentages of type H vessels (HV/TV; %) were calculated. Emcn antibody was purchased from Santa Cruz Biotechnology (Santa Cruz, USA). CD31 antibody and all secondary antibodies were obtained from Abcam.

Enzyme-linked immunosorbent assay (ELISA)

The concentrations of PDGF-BB and VEGF in the supernatant of bone marrow or in the CM were measured using a commercial Mouse PDGF-BB ELISA Kit (Cusabio, Wuhan, China) and a Mouse VEGF ELISA Kit (Multi Sciences LTD., Hangzhou, China) according to the protocol provided by the manufacturer. The optical density of each well was determined using a microplate reader (Bio-Rad 680, Hercules, USA) set to 450 nm. Wavelength correction was set to 570 nm. The protein concentration for each sample was calculated according to the standard curve.

Statistical analysis

All data are presented as mean ± standard deviation (SD). Two tailed Student's t-test was used to compare means between two groups. Analyses were performed using GraphPad Prism software and the differences were judged to be statistically significant when $P < 0.05$.

Results

Harmine increases the number of preosteoclasts and the production of PDGF-BB

To examine the effects of harmine on osteoclastogenesis and the production of PDGF-BB, osteoclast precursor cell line RAW264.7 cells were induced by the osteoclastogenic factor RANKL and treated with harmine or vehicle (DMSO) for 7 days. The expression levels of genes responsible for osteoclast terminal differentiation were assessed by qRT-PCR analysis. The results showed that RNAKL treatment caused significant increases in *Atp6v0d2* and *Ctsk* mRNA levels compared with the un-induced group, but the effect was markedly repressed by harmine (**Figure 1A-B**). However, *Pdgf-bb* expression was most abundant in harmine-treated cells (**Figure 1C**). TRAP staining revealed that RAW264.7 cells cultured with RANKL exhibited a large amount of TRAP$^+$ mononuclear preosteoclasts and multinucleated osteoclasts, whereas harmine treatment inhibited osteoclast formation and caused the accumulation of preosteoclasts (**Figure 1D-F**). As evidenced by ELISA, the concentration of PDGF-BB in CM from RNAKL-induced cells was much higher than that in the un-induced group, and harmine treatment resulted in a further increase of PDGF-BB production (**Figure 1G**). Our results suggest that harmine augments the production of PDGF-BB by increasing the number of preosteoclasts.

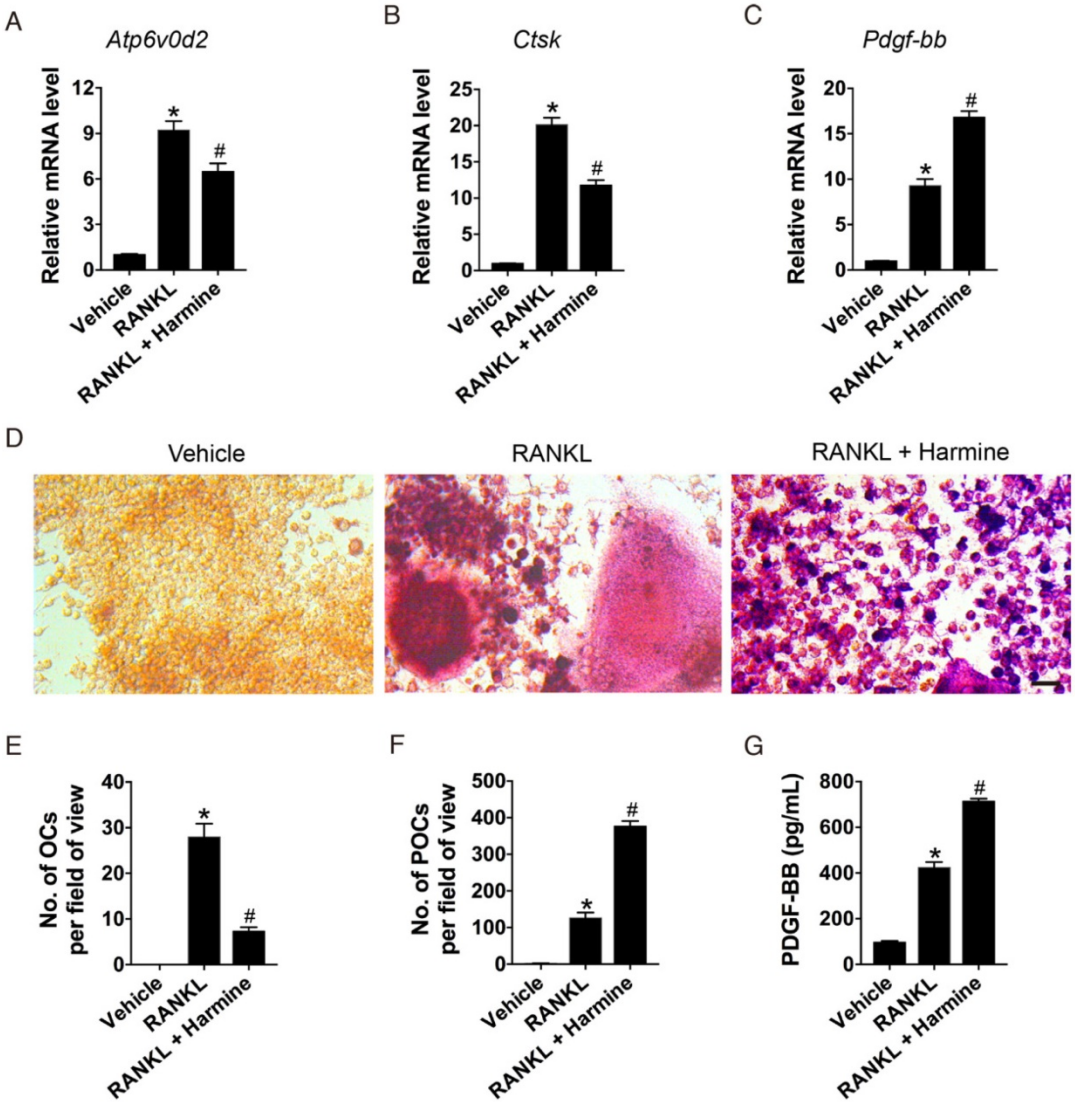

Figure 1. Harmine increases the number of preosteoclasts and the production of PDGF-BB. (A-C) qRT-PCR analysis of *Atp6v0d2*, *Ctsk* and *Pdgf-bb* expression levels relative to *Gapdh* in RAW264.7 cells treated with vehicle (DMSO), RANKL and RANKL + harmine. n = 4 per group. **(D)** Representative images of TRAP staining showing osteoclast and preosteoclast formation from RAW264.7 cells treated with vehicle, RANKL and RANKL + harmine. Scale bar: 50 μm. **(E-F)** Quantification of TRAP$^+$ osteoclasts (OCs) and preosteoclasts (POCs). n = 3 per group. **(G)** Detection of PDGF-BB concentration in conditioned media (CM) from RAW264.7 cells treated with vehicle, RANKL and RANKL + harmine by ELISA. n = 5 per group. *P < 0.05 vs. un-induced group (RAW264.7 cells treated with harmine vehicle DMSO), #P < 0.05 vs. RANKL group (RAW264.7 cells treated with RANKL + DMSO).

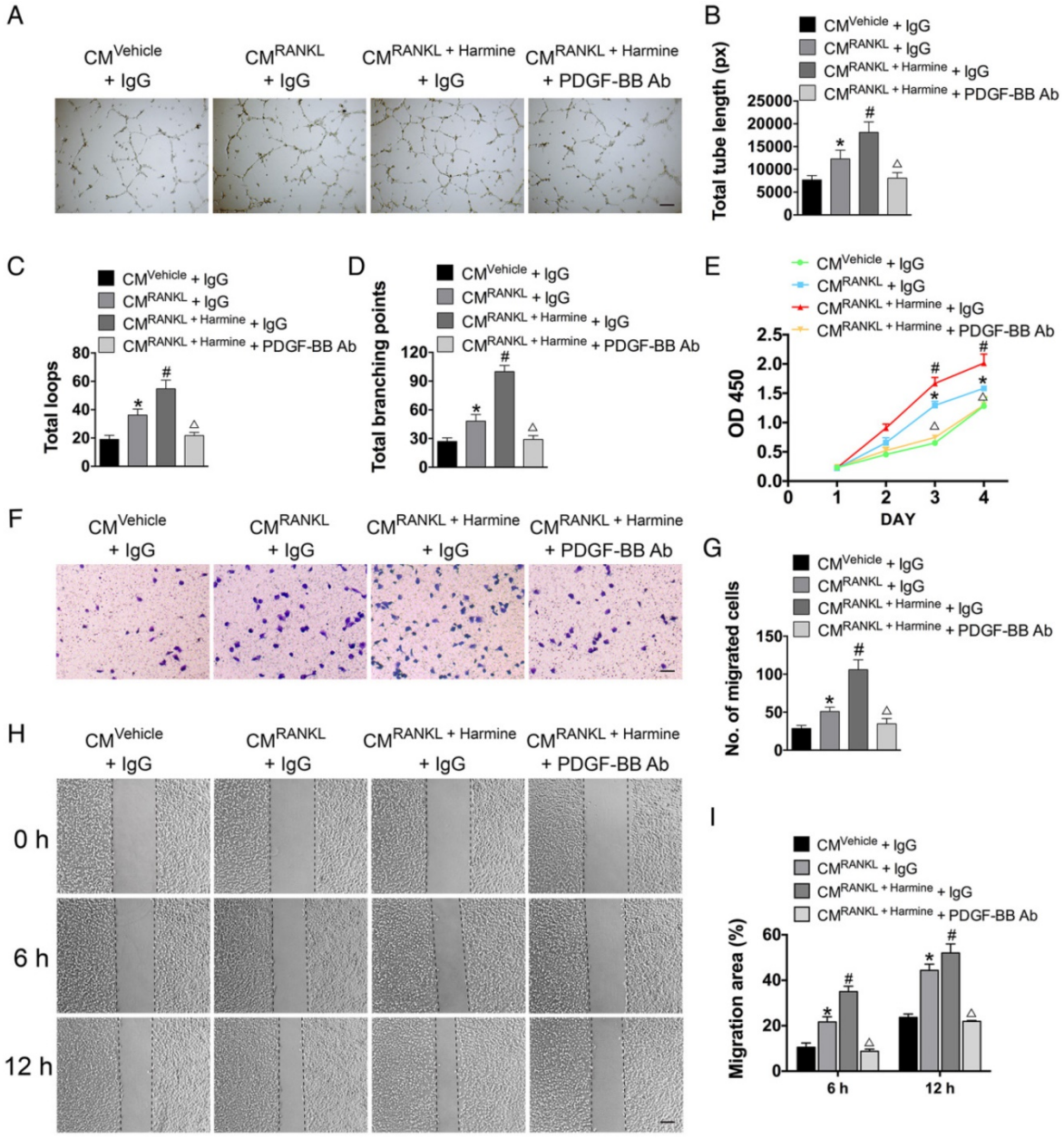

Figure 2. Harmine augments the pro-angiogenic effects of preosteoclasts on endothelial cells. (A-D) Representative images and quantification of tube formation in HMECs stimulated with CM from different groups and PDGF-BB-neutralizing antibody or IgG isotype control antibody. Scale bar: 200 μm. n = 5 per group. **(E)** CCK-8 analysis of HMEC proliferation in different treatment groups. n = 4 per group. **(F-I)** HMEC motility in different treatment groups was evaluated by the transwell migration assay **(F-G)** (Scale bar: 100 μm) and the scratch wound assay **(H-I)** (Scale bar: 200 μm). n = 3 per group. **P* < 0.05 vs. $CM^{Vehicle}$ + IgG group, #*P* < 0.05 vs. CM^{RANKL} + IgG group, Δ*P* < 0.05 vs. $CM^{RANKL + Harmine}$ + IgG group.

Harmine promotes preosteoclast PDGF-BB-induced angiogenesis

To test the effects of harmine on preosteoclast-induced angiogenesis, HMECs were incubated with the CM from RAW264.7 cells stimulated by RANKL or RANKL + harmine for a series of angiogenesis-related functional assays. As shown in **Figure 2A**, HMECs treated with the CM from RANKL-stimulated RAW264.7 cells formed higher number of capillary tube-like structures on Matrigel compared with those treated with CM from un-induced cells; once the RANKL-induced cells were additionally treated with harmine, the pro-angiogenic effect of their CM was further enhanced. To verify the role of PDGF-BB in this process, PDGF-BB-neutralizing antibodies were added to the CM from RANKL + harmine-stimulated RAW264.7 cells and the CM-induced positive effect on tube formation was markedly reduced (**Figure 2A**). Quantitative measurements revealed that the CM from RANKL-stimulated RAW264.7 cells increased the total tube

length, total loops and total branching points compared to controls, and the CM from RANKL + harmine group exhibited much stronger pro-angiogenic effect on HMECs (**Figure 2B-D**). However, this effect was blocked by neutralizing antibodies against PDGF-BB (**Figure 2B-D**). CCK-8 analysis showed that HMEC proliferation was elevated in response to CM from RANKL-induced RAW264.7 cells and the proliferation of HMECs was stimulated to the relatively greatest extent when exposed to CM from RANKL + harmine-treated cells (**Figure 2E**). Once PDGF-BB-neutralizing antibodies were added to the CM from RANKL + harmine-treated cells, their positive effect on HMEC proliferation was reduced (**Figure 2E**). As evidenced by the transwell assay (**Figure 2F-G**) and scratch wound assay (**Figure 2H-I**), the CM from the RANKL + harmine group resulted in the greatest increase in HMEC migration compared to all other groups, whereas this effect was attenuated by PDGF-BB inhibition. These findings indicate that harmine has the ability to promote preosteoclast PDGF-BB-induced angiogenesis.

We also assessed the direct effects of harmine on endothelial angiogenesis in order to exclude the impact of the possible residual harmine in CM on endothelial cell function. The results of tube formation assay (**Figure 3A-D**), CCK-8 assay (**Figure 3E**) and scratch wound assay (**Figure 3F-G**) revealed that HMECs cultured with harmine exhibited significantly lower activities in tube formation, proliferation and motility compared with vehicle (DMSO)-treated cells, suggesting that the stimulatory effects of CM from RANKL + harmine-treated RAW264.7 cells on endothelial angiogenesis are not mediated by the residual harmine.

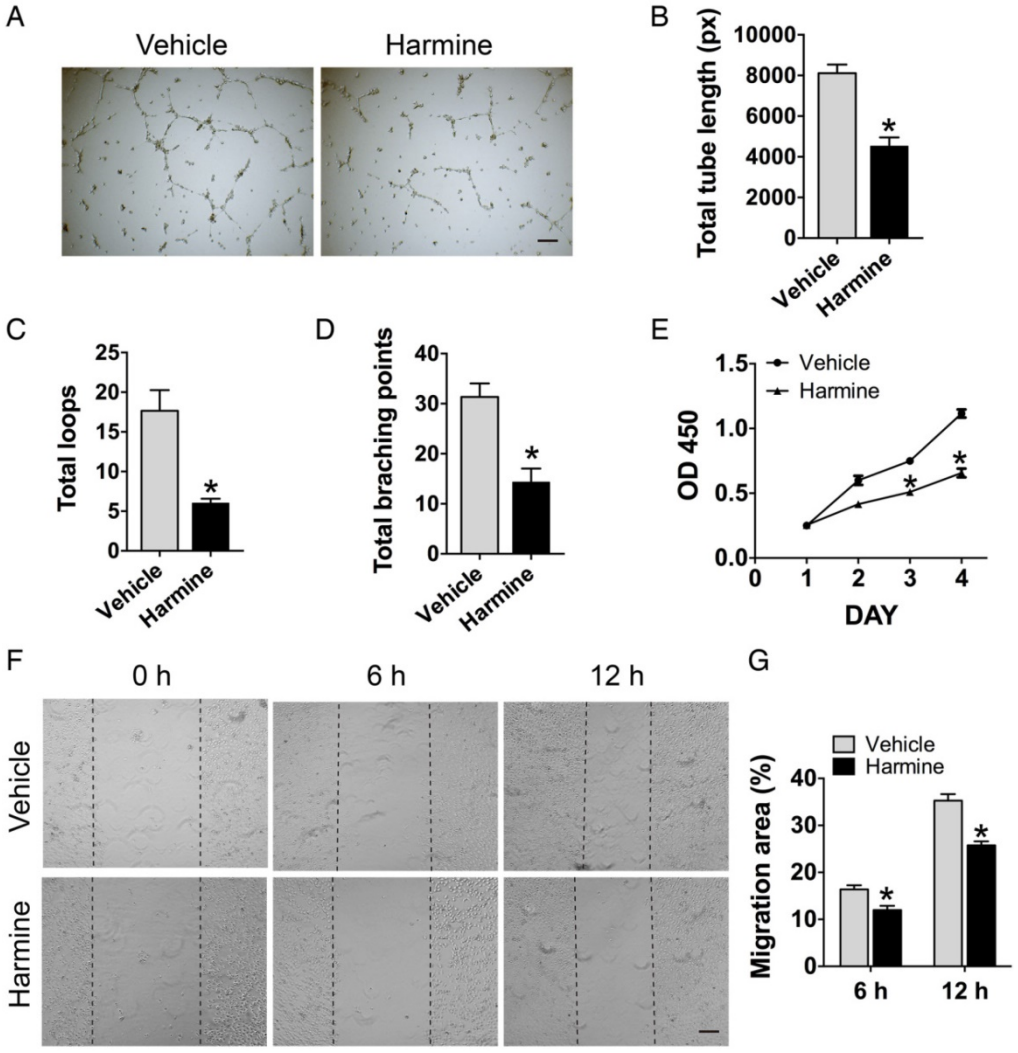

Figure 3. Direct treatment of harmine inhibits endothelial angiogenesis. (A) Representative images showing tube formation of HMECs on Matrigel. Scale bar: 200 μm. **(B-D)** Total tube length, total loops and total branching points were measured to quantify the ability of HMECs to form tubes. n = 5 per group. **(E)** Proliferation of HMECs analyzed by the CCK-8 analysis. n = 4 per group. **(F)** Migration of HMECs determined by the scratch wound assay. Scale bar: 200 μm. **(G)** Quantitative analysis of the rate of migration area in (F). n = 3 per group. * $P < 0.05$ vs. vehicle (DMSO) group.

Intragastric administration of harmine emulsion prevents bone loss in OVX mice

Previous reports have shown that intraperitoneal injection of harmine suppresses bone resorption *in vivo* [12], but also induces significant neurotoxic effects [13-15]. To minimize the undesired side effects, harmine was prepared into oil-in-water oral emulsion for our *in vivo* study. These emulsified particles exhibited a narrow particle size distribution with a mean diameter of 5.02 ± 1.79 μm (**Figure S1A-B**). We tested the pharmacokinetics, tissue distribution and toxicities of harmine emulsion administrated intragastrically in normal mice. The results showed that harmine was rapidly eliminated from serum ($t_{1/2}$ = 11.04 min; **Figure S1C**) and mainly distributed in stomach, intestine, liver, lung and bone marrow after administration (**Figure S1D**). No remarkable differences were found between harmine emulsion- and vehicle-treated mice, including daily behaviors (**Videos S1-2**) and the serum levels of liver (ALT and AST) and kidney (creatinine and BUN) function indicators (**Figure S2A-D**). However, the intraperitoneal injection of harmine solution into mice immediately caused serious neurological effects, such as acute uncontrollable action tremors, convulsions and rigidity (**Videos S3-4**). High levels of harmine accumulation in brain tissues in the solution group (**Figure S1E**) may be correlated with its neural toxicity. Our results suggest that the oral administration of harmine in an emulsion form reduces the neural toxicity of harmine and may be suitable for use *in vivo*.

To evaluate the effects of harmine emulsion on osteoporosis, OVX mice were generated and intragastrically administrated with harmine emulsion or vehicle (DMSO) for two months. **Figure 4A-B** show significantly smaller uterus size and lower uterus weight in OVX mice compared to sham-operated mice, which confirmed the success of OVX. μCT scanning revealed that OVX mice had markedly lower trabecular bone mass in the distal metaphysis of the femur than that in the sham group, but the intragastric administration of harmine to OVX mice attenuated bone loss (**Figure 4C**). Quantitative analyses of trabecular bone volume fraction (Tb. BV/TV), trabecular thickness (Tb. Th), number (Tb. N) and separation (Tb. Sp) confirmed the preventive efficacy of harmine on OVX-induced bone loss (**Figure 4D-G**). H&E staining showed plenty of fat vacuoles in bone marrow in OVX mice, while harmine treatment prevented the accumulation of fat cells (**Figure 5A-B**). Immunohistochemical staining for OCN revealed that osteogenic activity was slightly reduced in OVX mice, but remarkably increased when the OVX mice were treated with harmine (**Figure 5C-D**). TRAP staining showed a large number of osteoclasts on the trabecular bone surface in OVX mice. However, significantly reduced numbers of osteoclasts and enhanced numbers of preosteoclasts were observed in harmine-treated OVX mice (**Figure 5E-F**), suggesting an inhibitory role of harmine in the differentiation of preosteoclasts into osteoclasts, which was consistent with the results of our *in vitro* study. Our results indicate that the intragastric administration of harmine emulsion effectively protects against OVX-induced osteoporosis.

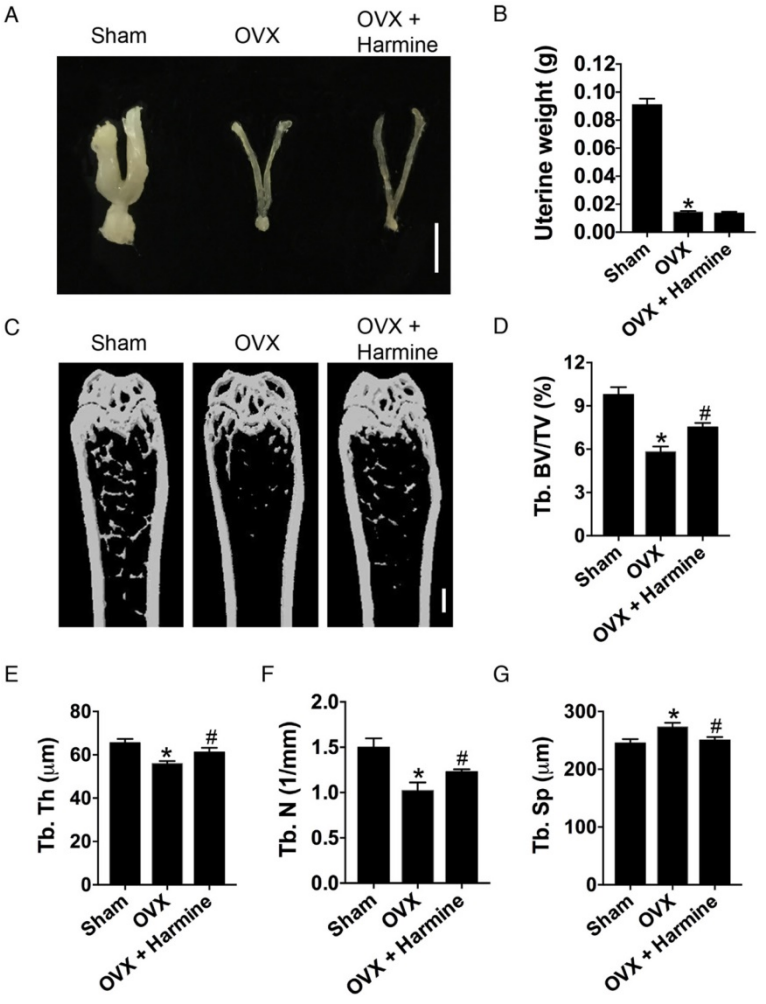

Figure 4. Intragastric administration of harmine emulsion prevents bone loss induced by OVX. (A) Representative images showing uterine morphology from sham-operated, OVX and OVX mice with harmine treatment. Scale bar: 0.5 cm. **(B)** Uterine weight in different treatment groups. n = 5 per group. **(C-G)** Representative μCT images **(C)** and quantitative μCT analysis **(D-G)** of trabecular bone mass and microarchitecture in femora from sham, OVX and OVX + harmine mice. Scale bar: 1 mm. n = 6-8 per group. **P* < 0.05 vs. sham group, #*P* < 0.05 vs. OVX group.

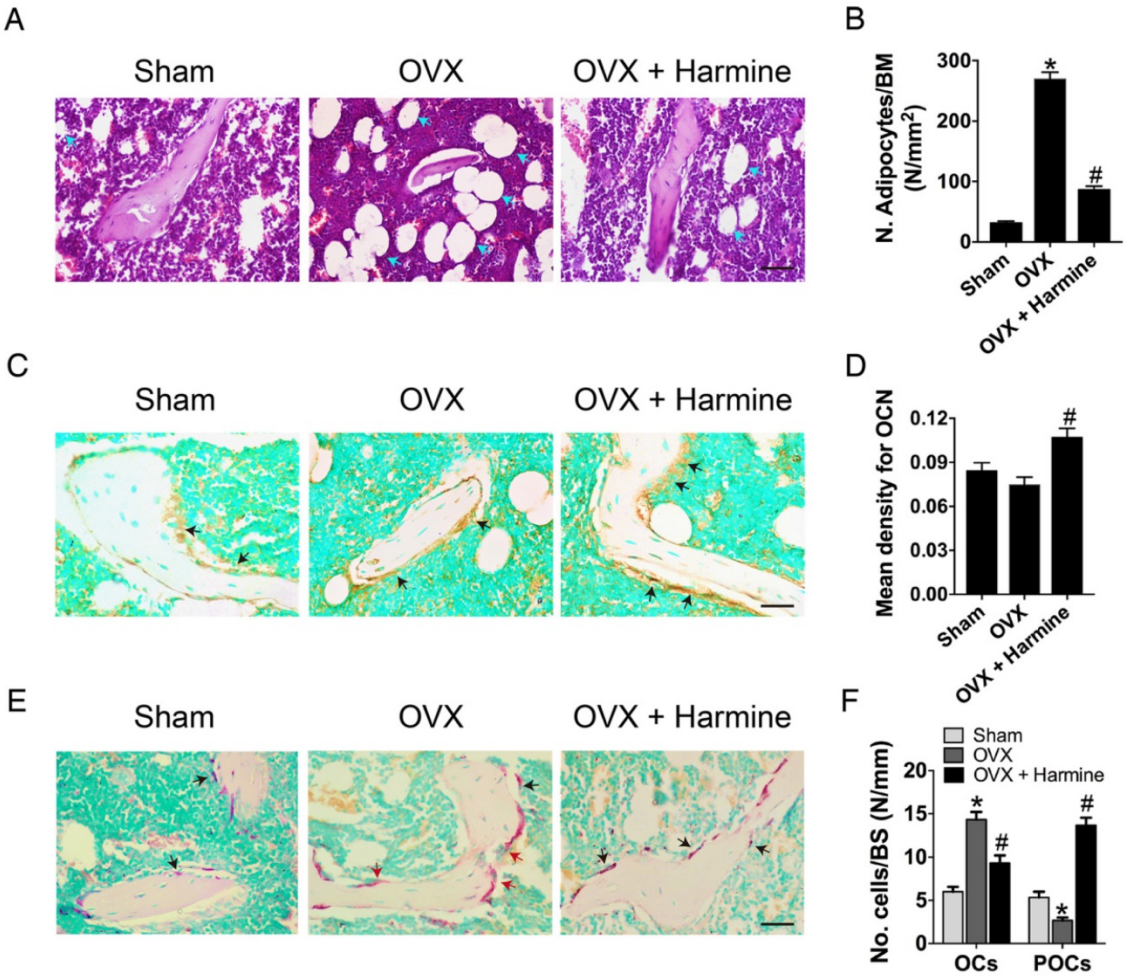

Figure 5. Harmine emulsion stimulates osteogenesis and represses osteoclast formation in OVX mice. (A-B) Representative H&E stained images **(A)** and quantification of adipocytes **(B)** in distal femoral metaphysis regions from sham, OVX and OVX + harmine mice. Blue arrows indicate adipocytes. Scale bar: 50 μm. n = 4 per group. BM: bone marrow. **(C)** Representative images of OCN immunostaining in femora from sham, OVX and OVX + harmine mice. Black arrows indicate OCN-positive areas. Scale bar: 50 μm. **(D)** Quantification of the mean intensity for the OCN immunostaining in different treatment groups. n = 4 per group. **(E)** TRAP staining of femora from sham, OVX and OVX + harmine mice. Red arrows indicate OCs and black arrows indicate POCs. Scale bar: 50 μm. **(F)** Quantification of TRAP$^+$ OCs and POCs per bone surface (BS) in different treatment groups. n = 3 per group. *$P < 0.05$ vs. sham group, #$P < 0.05$ vs. OVX group.

Intragastric administration of harmine induces type H vessel formation

Next, CD31 and Emcn immunofluorescence double staining was performed to verify the effects of harmine on type H blood vessel formation. As shown in **Figure 6A-B**, OVX mice had a significantly lower proportion of type H vessels in the metaphysis of the femur compared to sham-operated mice, which was consistent with our previous report [9]. Surprisingly, the intragastric administration of harmine to OVX mice led to a prominent increase in the percentage of this specific vessel subtype to a similar extent as in sham-operated mice. The bone marrow concentrations of PDGF-BB (**Figure 6C**) and VEGF (**Figure 6D**), as detected by ELISA, were dramatically decreased in mice who underwent OVX. In contrast, these pro-angiogenic factors in OVX mice treated with harmine emulsion were markedly elevated. These data, along with our *in vitro* results, suggest that the promotion of preosteoclast-induced angiogenesis may be an important mechanism by which harmine prevents bone loss. Since our results showed that harmine treatment enhanced osteogenic differentiation of mesenchymal stem cells (MSCs) *in vitro* (**Figure S3**), a direct stimulation of osteogenesis may also contribute to harmine-induced inhibition of bone loss.

Discussion

Osteoporosis is a major chronic disease worldwide in an aging population and frequently leads to fragility fractures, which bring about low quality of life, increased mortality and high healthcare costs [19]. Bisphosphonates and denosumab are the most regular drugs for clinical treatment of osteoporosis, which strongly inhibit resorption of bone, but also suppress ossification and angiogenesis, resulting in atypical femoral fractures and

osteonecrosis of the jaw [19-21]. Thus, it is required to develop more ideal drugs for the prevention and treatment of osteoporosis. In the present study, we demonstrated that the intragastric administration of harmine emulsion effectively evoked bone-sparing effects in OVX-induced osteoporotic mice, as defined by enhanced trabecular bone mass and osteogenic responses, as well as decreased osteoclast formation, suggesting the potential utility of harmine as a drug for postmenopausal osteoporosis.

The use of harmine as a multi-purpose traditional medicine has been translated into several commercial applications [10]. Harmine has many traditional medicinal uses and pharmacological activities such as anti-inflammatory, anti-parasitic and anti-tumor properties [10, 22-26]. An investigation on the effect of harmine on osteoclastogenesis of RAW264.7 cells showed that harmine could inhibit RANKL-induced multinucleated osteoclast formation and prevent bone resorption in both cell and bone tissue cultures [12]. Intraperitoneal administration with harmine was able to suppress OVX-induced bone loss in mice [12]. However, it should be noted that intraperitoneal injection of harmine could cause serious central nervous system side effects [13-15, 26], which impede the development of harmine toward wider clinical applications [26]. In this study, we generated an oil-in-water harmine emulsion and found that the oral administration of harmine in emulsion form reduced harmine accumulation in the mouse brain. All the mice oral gavaged with harmine emulsion did not demonstrate abnormal neurological behaviors, but the mice intraperitoneally injected with harmine solution showed high levels of harmine accumulation in the brain and exhibited neurotoxic actions immediately. Consistently, no signs of neurotoxicity were observed in OVX mice intragastrically administrated with harmine emulsion during the experiments. Following oral administration, certain amounts of harmine were detected in mouse bone marrow, which may explain the bone-protective effects of harmine emulsion on OVX mice. Thus, harmine emulsion may be used as a promising and safer therapeutic agent for osteoporosis, which needs to be verified by clinical trials in the future.

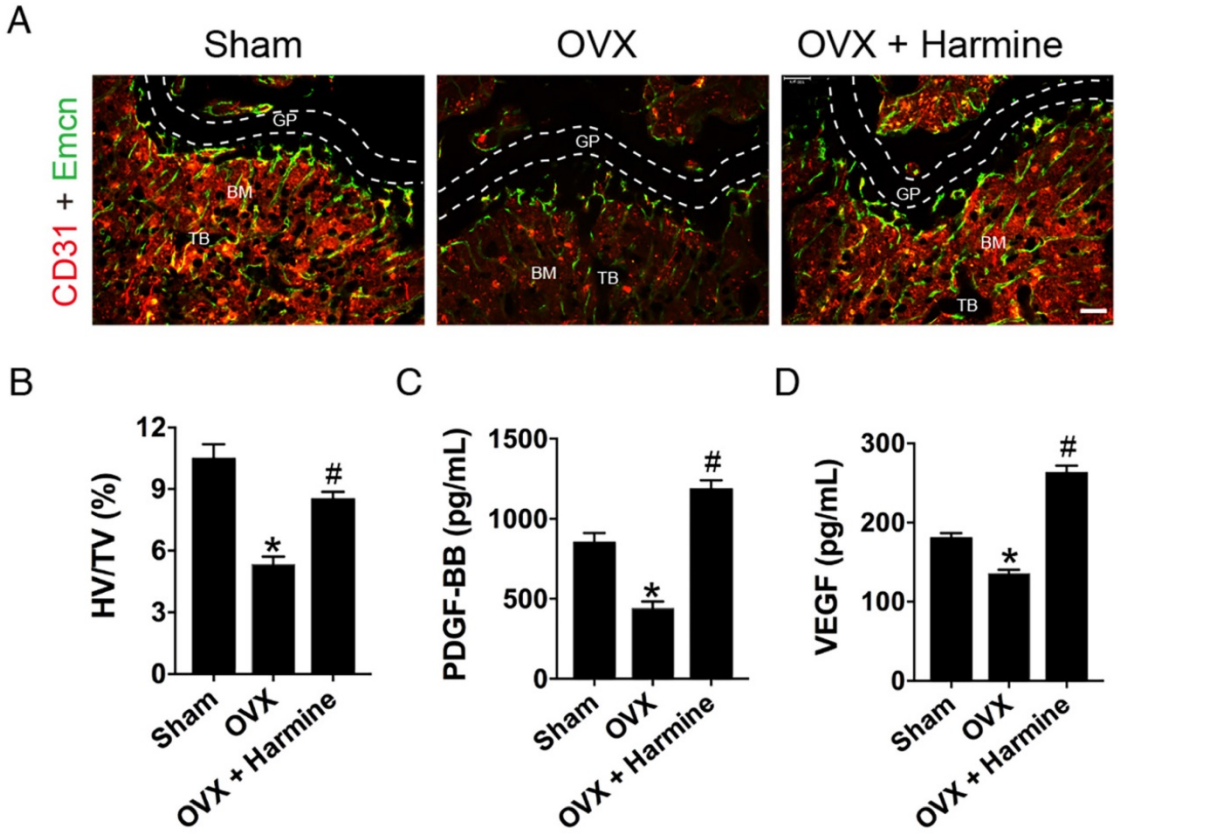

Figure 6. Harmine emulsion induces type H vessel formation and PDGF-BB production in OVX mice. (A) Representative images of CD31 (red) and Emcn (green) immunostaining in femora from sham, OVX and OVX + harmine mice. BM: bone marrow; GP: growth plate; TB: trabecular bone. Scale bar: 100 μm. **(B)** Quantification of the ratio of type H vessel (HV; yellow) in different treatment groups. n = 4 per group. TV: total vessels. **(C-D)** Bone marrow concentrations of PDGF-BB and VEGF from sham, OVX and OVX + harmine mice were detected by ELISA. n = 4 per group. **P* < 0.05 vs. sham group, #*P* < 0.05 vs. OVX group.

The importance of angiogenesis in the maintenance of bone has been established. Bone formation requires new blood vessel formation and endothelial cell-derived molecular signals [3-5]. The osteogenesis-promoting effect of the bone vasculature in physiological settings was recently attributed to type H blood vessels [6, 7]. We and others demonstrated that the relative abundance of this distinct vessel subtype is associated with bone formation and bone loss [6-9]. Moreover, we found that PDGF-BB secreted by preosteoclasts could promote formation of the specific vessels to induce the coupling of angiogenesis with bone formation [9], suggesting that PDGF-BB may be a potential therapeutic target for osteoporosis.

In the present study, we found that harmine inhibited the fusion of preosteoclasts into osteoclasts, leading to an accumulation of preosteoclasts and a significant increase of secreted PDGF-BB in the CM. As expected, endothelial cells incubated with the CM exhibited remarkably enhanced angiogenic activities, whereas the effects were blocked by addition of the PDGF-BB-neutralizing antibodies. *In vivo*, we found that the number of type H blood vessels and the concentration of bone marrow PDGF-BB in osteoporotic mice were markedly increased after harmine administration. To the best of our knowledge, this study is the first to show that harmine can augment angiogenesis by increasing preosteoclast PDGF-BB activity. However, it should be noted that harmine has the ability to directly regulate angiogenesis. Previous studies reported that direct treatment of harmine could reduce proliferation, migration and tube formation of endothelial cells, as well as inhibit microvessel outgrowth from the rat aortic ring [27, 28]. Consistently, results from our study also determined that harmine significantly inhibited angiogenic responses of endothelial cells *in vitro*, which seemed to be inconsistent with our *in vivo* results showing that harmine augmented angiogenesis in bone. The paradoxical results suggest that the pro-angiogenic effect of harmine is mediated through an indirect mechanism. The above data, when taken together, indicate that the promotion of preosteoclast PDGF-BB-induced angiogenesis may be a key mechanism by which harmine accelerates bone formation and prevents bone loss induced by OVX.

In this study, we found that exposure of MSCs to harmine enhanced osteogenesis of MSCs *in vitro*. Thus, a direct promotion of osteogenesis may also be an important mechanism by which harmine prevents osteoporosis. However, the detailed molecular mechanism by which harmine promotes osteogenesis was not assessed in our study. Studies have revealed that excessive adipocyte formation in the bone marrow cavity is an important factor in the development of osteoporosis and this occurs due to a shift in the differentiation of MSCs to favour adipocyte formation at the expense of forming osteoblasts [29-32]. Herein, we found that harmine treatment markedly inhibited the accumulation of fat cells in the bone marrow of OVX mice, suggesting that harmine may reverse the differentiation fate of MSCs from adipogenesis to osteogenesis, which requires further investigation.

In summary, our findings demonstrate that the intragastric administration of harmine emulsion facilitates type H blood vessels and bone formation in osteoporotic mice. The underlying mechanism may be the inhibition of osteoclast formation and the promotion of preosteoclast PDGF-BB-induced angiogenesis, as harmine can block the fusion of preosteoclasts into osteoclasts and augment the pro-angiogenic effects of preosteoclasts by increasing PDGF-BB production *in vitro*. Our study suggests that harmine may represent a promising drug for the prevention and treatment of osteoporosis.

Abbreviations

ALT: alanine aminotransferase; AST: aspartate aminotransferase; BUN: blood urea nitrogen; CCK-8: cell counting kit-8; CM: conditioned media; DMEM: dulbecco's modified eagle medium; DMSO: dimethyl sulfoxide; EDTA: ethylene diamine tetraacetic acid; ELISA: enzyme-linked immunosorbent assay; H&E: hematoxylin and eosin; MSCs: mesenchymal stem cells; OCN: osteocalcin; OVX: ovariectomy; PDGF-BB: platelet-derived growth factor-BB; qRT-PCR: quantitative real-time PCR; RANKL: receptor activator for nuclear factor-κB ligand; SD: standard deviation; Tb. BV/TV: trabecular bone volume fraction; Tb. N: trabecular number; Tb. Sp: trabecular separation; Tb. Th: trabecular thickness; TRAP: tartrate-resistant acid phosphatase; μCT: microcomputed tomography; VEGF: vascular endothelial growth factor.

Acknowledgements

This work was supported by the Excellent Young Scientist Award of National Natural Science Foundation of China (Grant No. 81522012), the National Natural Science Foundation of China (Grant No. 81670807, 81600699, 81702237, 81701383, 81400858), the Thousand Youth Talents Plan of China (Grant No. D1119003), the Hunan Youth Talent Project (Grant No. 2016RS3021), the Innovation Driven Project of Central South University (2016CX028), the Youth Foundation of Xiangya Hospital in Central South University (Grant No. 2016Q10), the Fundamental Research Funds for the

Central Universities of Central South University (Grant No. 2017zzts032, 2017zzts014), the Hunan Province Natural Science Foundation of China (Grant No. 2017JJ3501), the China Postdoctoral Science Foundation (Grant No. 2017M612596, 2017M622614) and the Natural Science Foundation for Distinguished Yong Scholars of Guangdong Province (2016A030306051).

Author Contributions

HX and CYC conceived and designed the experiments. JH, HY and SSR performed the experiments. HX, CYC and JH wrote the manuscript. JH, CYC and HY analyzed the data and prepared all the figures. YJT and JL helped with the biochemical experiment. PLX, XC, ZXW, JC, YH, ZZL, BW, XKH and THC provided technical support. All authors reviewed and agreed upon the manuscript.

Supplementary Material

Supplementary figures and methods.
http://www.thno.org/v08p2435s1.pdf

Competing Interests

The authors have declared that no competing interest exists.

References

1. Tomlinson RE, Silva MJ. Skeletal Blood Flow in Bone Repair and Maintenance. Bone Res. 2013; 1: 311-22.
2. Yang M, Li CJ, Sun X, Guo Q, Xiao Y, Su T, et al. MiR-497 approximately 195 cluster regulates angiogenesis during coupling with osteogenesis by maintaining endothelial Notch and HIF-1alpha activity. Nat Commun. 2017; 8: 16003.
3. Huang B, Wang W, Li Q, Wang Z, Yan B, Zhang Z, et al. Osteoblasts secrete Cxcl9 to regulate angiogenesis in bone. Nat Commun. 2016; 7: 13885.
4. Ramasamy SK, Kusumbe AP, Schiller M, Zeuschner D, Bixel MG, Milia C, et al. Blood flow controls bone vascular function and osteogenesis. Nat Commun. 2016; 7: 13601.
5. Stegen S, van Gastel N, Carmeliet G. Bringing new life to damaged bone: the importance of angiogenesis in bone repair and regeneration. Bone. 2015; 70: 19-27.
6. Kusumbe AP, Ramasamy SK, Adams RH. Coupling of angiogenesis and osteogenesis by a specific vessel subtype in bone. Nature. 2014; 507: 323-8.
7. Ramasamy SK, Kusumbe AP, Wang L, Adams RH. Endothelial Notch activity promotes angiogenesis and osteogenesis in bone. Nature. 2014; 507: 376-80.
8. Wang L, Zhou F, Zhang P, Wang H, Qu Z, Jia P, et al. Human type H vessels are a sensitive biomarker of bone mass. Cell Death Dis. 2017; 8: e2760.
9. Xie H, Cui Z, Wang L, Xia Z, Hu Y, Xian L, et al. PDGF-BB secreted by preosteoclasts induces angiogenesis during coupling with osteogenesis. Nat Med. 2014; 20: 1270-8.
10. Patel K, Gadewar M, Tripathi R, Prasad SK, Patel DK. A review on medicinal importance, pharmacological activity and bioanalytical aspects of beta-carboline alkaloid "Harmine". Asian Pac J Trop Biomed. 2012; 2: 660-4.
11. Egusa H, Doi M, Saeki M, Fukuyasu S, Akashi Y, Yokota Y, et al. The small molecule harmine regulates NFATc1 and Id2 expression in osteoclast progenitor cells. Bone. 2011; 49: 264-74.
12. Yonezawa T, Hasegawa S, Asai M, Ninomiya T, Sasaki T, Cha BY, et al. Harmine, a beta-carboline alkaloid, inhibits osteoclast differentiation and bone resorption in vitro and in vivo. Eur J Pharmacol. 2011; 650: 511-8.
13. Aricioglu F, Yillar O, Korcegez E, Berkman K. Effect of harmane on the convulsive threshold in epilepsy models in mice. Ann N Y Acad Sci. 2003; 1009: 190-5.
14. Guan Y, Louis ED, Zheng W. Toxicokinetics of tremorogenic natural products, harmane and harmine, in male Sprague-Dawley rats. J Toxicol Environ Health A. 2001; 64: 645-60.
15. Sourkes TL. "Rational hope" in the early treatment of Parkinson's disease. Can J Physiol Pharmacol. 1999; 77: 375-82.
16. Zhang J, Chen C, Hu B, Niu X, Liu X, Zhang G, et al. Exosomes Derived from Human Endothelial Progenitor Cells Accelerate Cutaneous Wound Healing by Promoting Angiogenesis Through Erk1/2 Signaling. Int J Biol Sci. 2016; 12: 1472-87.
17. Xie H, Xie PL, Luo XH, Wu XP, Zhou HD, Tang SY, et al. Omentin-1 exerts bone-sparing effect in ovariectomized mice. Osteoporos Int. 2012; 23: 1425-36.
18. Liu T, Qin AP, Liao B, Shao HG, Guo LJ, Xie GQ, et al. A novel microRNA regulates osteoclast differentiation via targeting protein inhibitor of activated STAT3 (PIAS3). Bone. 2014; 67: 156-65.
19. Rachner TD, Khosla S, Hofbauer LC. Osteoporosis: now and the future. Lancet. 2011; 377: 1276-87.
20. Black DM, Bauer DC, Schwartz AV, Cummings SR, Rosen CJ. Continuing bisphosphonate treatment for osteoporosis—for whom and for how long? N Engl J Med. 2012; 366: 2051-3.
21. Cosman F, Crittenden DB, Adachi JD, Binkley N, Czerwinski E, Ferrari S, et al. Romosozumab Treatment in Postmenopausal Women with Osteoporosis. N Engl J Med. 2016; 375: 1532-43.
22. Liu X, Li M, Tan S, Wang C, Fan S, Huang C. Harmine is an inflammatory inhibitor through the suppression of NF-kappaB signaling. Biochem Biophys Res Commun. 2017; 489: 332-8.
23. Di Giorgio C, Delmas F, Ollivier E, Elias R, Balansard G, Timon-David P. In vitro activity of the beta-carboline alkaloids harmane, harmine, and harmaline toward parasites of the species Leishmania infantum. Exp Parasitol. 2004; 106: 67-74.
24. Lala S, Pramanick S, Mukhopadhyay S, Bandyopadhyay S, Basu MK. Harmine: evaluation of its antileishmanial properties in various vesicular delivery systems. J Drug Target. 2004; 12: 165-75.
25. Zhang H, Sun K, Ding J, Xu H, Zhu L, Zhang K, et al. Harmine induces apoptosis and inhibits tumor cell proliferation, migration and invasion through down-regulation of cyclooxygenase-2 expression in gastric cancer. Phytomedicine. 2014; 21: 348-55.
26. Li S, Wang A, Gu F, Wang Z, Tian C, Qian Z, et al. Novel harmine derivatives for tumor targeted therapy. Oncotarget. 2015; 6: 8988-9001.
27. Dai F, Chen Y, Song Y, Huang L, Zhai D, Dong Y, et al. A natural small molecule harmine inhibits angiogenesis and suppresses tumour growth through activation of p53 in endothelial cells. PloS One. 2012; 7: e52162.
28. Hamsa TP, Kuttan G. Harmine inhibits tumour specific neo-vessel formation by regulating VEGF, MMP, TIMP and pro-inflammatory mediators both in vivo and in vitro. Eur J Pharmacol. 2010; 649: 64-73.
29. Jing H, Liao L, An Y, Su X, Liu S, Shuai Y, et al. Suppression of EZH2 Prevents the Shift of Osteoporotic MSC Fate to Adipocyte and Enhances Bone Formation During Osteoporosis. Mol Ther. 2016; 24: 217-29.
30. Lu Q, Liu H, Cao T. Efficient isolation of bone marrow adipocyte progenitors by silica microbeads incubation. Stem Cells Dev. 2013; 22: 2520-31.
31. Chen CY, Tseng KY, Lai YL, Chen YS, Lin FH, Lin S. Overexpression of Insulin-Like Growth Factor 1 Enhanced the Osteogenic Capability of Aging Bone Marrow Mesenchymal Stem Cells. Theranostics. 2017; 7: 1598-611.
32. Guo Q, Chen Y, Guo L, Jiang T, Lin Z. miR-23a/b regulates the balance between osteoblast and adipocyte differentiation in bone marrow mesenchymal stem cells. Bone Res. 2016; 4: 16022.